UCLA
UCLA Previously Published Works

Title
Effects of dietary omega-3 fatty acids on orthotopic prostate cancer progression, tumor associated macrophages, angiogenesis and T-cell activation—dependence on GPR120

Permalink
https://escholarship.org/uc/item/7x46t64r

Journal
Prostate Cancer and Prostatic Diseases, 25(3)

ISSN
1365-7852

Authors
Liang, Pei
Henning, Susanne M
Grogan, Tristan
et al.

Publication Date
2022-09-01

DOI
10.1038/s41391-021-00440-2

Peer reviewed

Effects of dietary omega-3 fatty acids on orthotopic prostate cancer progression, tumor associated macrophages, angiogenesis and T-cell activation—dependence on GPR120

Pei Liang[1], **Susanne M. Henning**[1], **Tristan Grogan**[2], **David Elashoff**[2], **Huihui Ye**[3], **Pinchas Cohen**[4], **William J. Aronson**[1,5]

[1]Department of Urology, David Geffen School of Medicine, University of California Los Angeles, Los Angeles, CA, USA.

[2]Department of Medicine Statistics Core, David Geffen School of Medicine, University of California, Los Angeles, Los Angeles, CA, USA.

[3]Department of Pathology, David Geffen School of Medicine, University of California Los Angeles, Los Angeles, CA, USA.

[4]Leonard Davis School of Gerontology, University of Southern California, Los Angeles, CA, USA.

[5]VA Medical Center Greater Los Angeles Healthcare System, Los Angeles, CA, USA.

Abstract

BACKGROUND: The antiprostate cancer effects of dietary ω-3 fatty acids (FAs) were previously found to be dependent on host G-protein coupled receptor 120 (GPR120). Using an orthotopic tumor model and an ex-vivo model of bone marrow derived M2-like macrophages, we sought to determine if ω-3 FAs inhibit angiogenesis and activate T-cells, and if these effects are dependent on GPR120.

METHODS: Gausia luciferase labeled MycCaP prostate cancer cells (MycCaP-Gluc) were injected into the anterior prostate lobe of FVB mice. After established tumors were confirmed by blood luminescence, mice were fed an ω-3 or ω-6 diet. Five weeks after tumor injection, tumor weight, immune cell infiltration and markers of angiogenesis were determined. An ex-vivo co-culture model of bone marrow derived M2-like macrophages from wild-type or GPR120 knockout mice with MycCap prostate cancer cells was used to determine if docosahexanoic acid (DHA, ω-3 FA) inhibition of angiogenesis and T-cell activation is dependent on macrophage GPR120.

RESULTS: Feeding an ω-3 diet significantly reduced orthotopic MycCaP-Gluc tumor growth relative to an ω-6 diet. Tumors from the ω-3 group had decreased M2-like macrophage infiltration and decreased expression of angiogenesis factors. DHA significantly inhibited M2 macrophage-induced endothelial tube formation and reversed M2 macrophage-induced T-cell suppression, and these DHA effects were mediated, in part, by M2 macrophage GPR120.

CONCLUSION: Omega-3 FAs delayed orthotopic tumor growth, inhibited M2-like macrophage tumor infiltration, and inhibited M2-like macrophage-induced angiogenesis and T-cell suppression. Given the central role of M2-like macrophages in prostate cancer progression, GPR120-dependent ω-3 FA inhibition of M2-like macrophages may play an important role in prostate cancer therapeutics.

INTRODUCTION

In numerous preclinical models, dietary ω-3 fatty acids (FAs) from fish oil delayed the development and progression of androgen sensitive and castrate resistant prostate cancer [1-8].

Epidemiologic studies, however, report varying results with regards to fish and ω-3 intake and risk of overall and aggressive prostate cancer [9-15]. In a prospective trial in men on active surveillance, higher prostate tissue eicosapentaenoic acid (EPA, ω-3) levels correlated with less upgrading on subsequent biopsies [16-18]. Likewise, a small prospective randomized preprostatectomy trial reported decreased proliferation (Ki-67 index) and decreased genetic risk score (cell cycle progression score) in malignant tissue in the prostatectomy specimens in men on an ω-3 FA based diet as compared to a Western diet [19].

There are a number of potential mechanisms for the anticancer effects of dietary ω-3 FAs [20]. In castration sensitive and resistant models, dietary ω-3 intake (as compared to ω-6 intake) decreased tumor infiltration of M2-like macrophages [5, 6]. M2-like macrophages play a key role in cancer progression through enhancing tumor invasion, angiogenesis, and immunosuppression [21-27]. In patients with advanced prostate cancer, M2-like macrophages make up the preponderance of immune cells in metastatic deposits and M2-like cells in the primary tumor are positively associated with aggressive disease [28-30].

The antiprostate cancer effects of dietary ω-3 FAs appear to be dependent on the presence of functional host GPR120, although the host cell type(s) responsible are yet to be defined [6]. GPR120 is a receptor for ω-3 FAs on macrophages and adipocytes [31, 32]. Specific GPR120 polymorphisms increase the risk of obesity and lung cancer, though associations with prostate cancer risk have not been reported [33, 34]. Of interest, a prospective trial in men with prostate cancer reported greater antiproliferative effects of an ω-3 based diet in patients with higher expression of GPR120 in prostate stroma, suggesting that GPR120 status may predict responsiveness to an ω-3 based diet [6].

Dietary ω-3 FAs delay prostate cancer progression in xenograft models in immunosuppressed mice, and in allograft and genetic immunocompetent mouse models

[1-6]. To date, dietary ω-3 FAs have not been tested in an orthotopic immunocompetent model. Orthotopic tumor growth occurs in the local microenvironment of the prostate and may represent a more physiologic model for angiogenesis and other biological pathways as compared to subcutaneous tumor models [35-37]. In the present study we examined if dietary ω-3 FAs delay prostate cancer progression in an orthotopic mouse model of prostate cancer. Through the use of an ex-vivo model incorporating bone marrow derived M2-like macrophages, we also sought to determine if ω-3 FAs inhibit angiogenesis, and activate T-cells, and if these effects are dependent on GPR120.

MATERIALS AND METHODS

Chemicals, reagents and diets

Docosahexaenoic acid (DHA) was obtained from Cayman Chemical (Ann Harbor, MI), RPMI and DMEM media and fetal bovine serum (FBS) from Invitrogen (Carlsbad, CA), and mouse interleukin 4 (IL-4) from Sigma Chemical (St Louis, MO, USA). Coelenterazine was purchased from MedChem Express (Monmouth Junction, NJ). Mouse diets were purchased from DYETS, Inc. (Bethlehem, PA). For the ω-6 diet, 30% of energy (134 g/kg) was provided by corn oil, and the ω-6 to ω-3 ratio was 18:1. For the ω-3 diet 30% of energy was provided by menhaden oil (134 g/kg) and the ω-6 to ω-3 ratio was 1:8 as previously described [5].

Establishment of MycCap cell line expression GLuc

Pre-made recombinant lentivirus containing LV-CMV-Gluc-Puro vector (SignaGen, MD) were transduced into MycCap cells for 72 h, then selected in the presence of puromycin (Invitrogen; Thermo Fisher Scientific, Inc.) for 14 days. The surviving cells were passaged and designated as MycCap-GLuc. GLuc functionality was tested in vitro by adding coelenterazine into MycCap-Gluc cells containing medium and signal was measured with IVIS Spectrum In Vivo Imaging System.

Animal husbandry, feeding protocol, and MycCaP orthotopic tumors

Male FVB mice (8 weeks old) were obtained from Jackson Laboratory (Bar Harbor, ME). The mice were housed individually to monitor and measure food intake. The experiments were approved by the UCLA Animal Research Committee, and the mice were cared for in accordance with institutional guidelines. Mice were acclimated for 7 days on a standard AIN-93G diet (DYETS, Bethlehem, PA). For the orthotopic allograft mouse model, prior to implantation of the tumor cells, blood was collected from the lateral saphenous vein and serum was stored. The orthotopic implantation was performed under surgically sterile conditions [38]. The mice were anesthetized with 2.5% isoflurane and 1.5% oxygen. The abdomen was cleaned three times with iodine solution (DifemPharma, Santiago, Chile) and 70% isopropanol. A 1-cm midline incision was made to expose the prostate gland. 2×10^5 MycCaP-Gluc cells in 20 μl of matrigel/phosphate-buffered saline (PBS) mixture (Corning Life Sciences, Corning, NY) in a 50-μl syringe with a 30-gauge needle were injected into the right anterior lobe. The abdominal wound was closed in one layer with 6/0 absorbable surgical suture (Ethicon, NJ). Blood was collected every week and luminescence measured by adding 5 μl of serum to 100 μl of coelenterizine working solution (100

μM). When luminescence readings reached 130 RLU, mice were assigned to the corn oil (D103702, DYET) ($N = 10$) or fish oil diet (D 103859, DYET) ($N = 12$) based on matching luminescence readings to achieve equal distribution between the two treatment groups. The number of mice was lower in the corn oil group because one mouse died prior to tumor implantation and in one mouse the tumor did not grow and the luminescence reading did not reach 130 RLU. The investigators were not blinded to the diets. All mice were euthanized with isoflurane 5 weeks after MycCaP-Gluc cells were implanted. Tumor tissue was weighed and rinsed with cold PBS. One portion of the tumor tissue was snap-frozen in liquid nitrogen, one portion fixed in neutral-buffered formalin (Sigma-Aldrich, St. Louis, MO), and one portion was used for flow cytometry. For the subcutaneous allograft mouse model 5×10^5 MycCap cells were mixed with matrigel and implanted into the flank of wild-type FVB mice under anesthesia as previously described [6, 7]. When tumor volumes reached 30–50 mm^3, mice were randomly assigned to either ω-3 or ω-6 diet. Mice were sacrificed 5 weeks after the tumor cells were injected and tumor tissue collected [6].

Flow cytometry analysis of immune cells

To prepare single-cell suspensions for flow cytometry, fresh tumor tissue was dissected into ~1–3mm^3 fragments and digested with 80 U/mL collagenase (Invitrogen) in DMEM containing 10% FBS for 1 h at 37 °C while shaking. After red blood cell (RBC) lysis, single-cell suspensions were filtered and incubated for 20 min on ice with the following antibodies (1:100): CD45-PE (Cat# 12-0451-81, eBioscience, San Diego, CA), F4/80-PE-Cy7 (Cat# 25-4801-82, eBioscience, San Diego, CA), CD11b-FITC (Cat# 553310, BD Biosciences San Jose, CA), CD206-APC (Cat# 141707, Biolegend, San Diego, CA),CD68-PerCP-Cy5.5 (Cat# 137009, Biolegend, San Diego, CA) for macrophages. Cells were washed with PBS before analysis on the BD LSR-II flow cytometer (Beckman Coulter).

mRNA isolation and quantitative PCR

Total RNA was extracted from tumors using RNeasy Mini kit (Qiagen, Valencia, CA) according to the manufacturer's protocol. The reverse-transcriptional PCR and quantitative real-time PCR were performed as previously described [39]. Briefly, first-strand cDNA was synthesized using MLV-Reverse Transcriptase and random hexamers (Promega, Madison, MI, USA). Quantitative PCR was performed using a Universal SYBR Green mastermix (Applied Biosystems, Grand Island, NY, USA) on CFX96 Real time PCR system (Bio-Rad, Hercules, CA, USA). Gene expression was calculated after normalization to GAPDH using the   CT method and expressed as relative mRNA level compared to control. Primer sequences used for SYBR-green RT-PCR are listed in Supplementary Table 1.

Generation of L929-conditioned media and M2-like bone marrow derived macrophages (BMDMs)

L929 cells (ATCC, Rockville, MD) were cultured in RPMI-1640 medium supplemented with 2 mmol/l l-glutamine, 100 U/ml penicillin, and 100 μg/ml streptomycin (Invitrogen, Carlsbad, CA), and 10% FBS. The conditioned media was collected from cells grown for 7 days.

The BMDMs were isolated from mouse bone marrow according to standard procedures with some modification [40]. In brief, bone marrow cells were removed from the femurs and tibias of FVB mice and cultured in Dulbecco's modified Eagle's medium supplemented with 10% FBS, with the addition of 20% L929-conditioned medium and 80% DMEM growth medium. Cells were cultured at 5×10^6 cells/well for 7 days with 5% CO2 and at 37 °C. For BMDM CM, cells were then treated with DHA for 24 h, and medium were collected as BMDM CM.

Co-culture and cell invasion assay

Mouse prostate cancer cell line MycCap was a gift from Dr. Lily Wu (UCLA, CA). All cell lines were used within 15 passages after thawing. Mycoplasma in the cell lines are being tested by PCR according to the manufacture's protocol (Applied Biological Materials Inc., Richmond, BC, Canada). MycCap cells were authenticated by measuring gene expression of human c-myc using qPCR and overexpression of c-myc was confirmed. The migration of BMDM cells was determined using Matrigel-coated (BD Biosciences, Bedford, MA, USA) inserts in 6-well plates. Briefly, BMDM (10^5) were added to the upper compartments in DMEM supplemented with 10% FBS, and MycCap cells (10^5) were seeded in the lower chambers. After BMDM had attached, medium from the upper chambers were replaced with serum-free DMEM and lower chamber were replaced with DMEM with 2% FBS containing DHA. After a 24 h continued co-culture with BMDM exposed to DHA, cells on the upper insert surface of the membrane were removed with cotton swabs and fixed with 4% paraformaldehyde. Invasive cells were stained with 0.5% crystal violet in 2% methanol, pictures taken with a microscope, and the number of invasive cells counted in four randomly selected fields. Viability of MycCap cells and cultured BMDMs was quantified using the MTT assay according to manufacturer's instructions (Promega, Madison, WI). Viability of MycCap cells was not significantly affected at 25 μM of DHA and BMDMs at 50 μM of DHA (Supplementary Fig. 1).

In vitro tube formation assay

Mouse endothelium 2H-11 and human endothelium HUVEC cells were purchased from ATCC (Rockville, MD). Unpolymerized Matrigel (BD Biosciences) was placed (50 μL/well) in a 96-well microtiter plate (0.32 cm^2/well) and polymerized for 1 h at 37 °C. Endothelial cells (1×10^4 per well) in 100 μL medium were layered onto the Matrigel surface. After a 4 h incubation in a 5% CO2 humidified atmosphere at 37 °C, tube formation was quantified on digital images collected from reverted phase-contrast light microscope (Olympus, Japan) and analyzed with image J (NIH).

CD8+T cell proliferation assay

CD8+ T cells were isolated from spleen cells of FVB mice using a CD8a+ T cell isolation kit (Miltenyi Biotec, CA). RBC contamination was removed using lysis buffer (Sigma-Aldrich, St. Louis, MO). 1×10^4 T cells/well were stimulated with anti-CD3 and anti-CD28 antibodies and cultured with condition medium from BMDMs in 96-well plates for 48 h, followed by the addition of BrdU for 24 h. After removing the medium, CD8+ T cells were fixed and DNA denatured. Anti-BrdU monoclonal antibody was added to mark the newly synthesized DNA. BrdU was quantified by the addition of conjugate and substrate

and measurement of absorbance at 450 nm according to the assay protocol (Millipore, Burlington, MA). Gene expression of INF-γ was analyzed by quantitative PCR.

Statistical analysis

Group size was determined based on data from previous mouse studies in our laboratory [6]. Quantitative measures (tumor luminescence reading and weight, gene expression, angiogenesis and cell migration in vitro analysis) were compared between the two groups (ω-3 and ω-6 diet) using two-tailed Student *t* test calculated by GraphPad Prism 6.0 software (GraphPad Software, La Jolla, CA). Using SAS software version 9.2 (Institute Inc, Cary, NC, USA), the normality assumption was assessed with the Shaprio–Wilk test. If the normality assumption was violated ($p < 0.05$), we used a log transformation prior to the *t*-test. If the equal variance assumption assessed by Levene's test was violated ($p < 0.05$), we used the Welch–Satterthwaite adjusted *t*-test, which does not assume equal variance between groups. The data from in vitro experiments are presented as mean ± standard deviation (SD), and mouse tumor growth evaluation in mean ± standard error of the mean (SEM). In vitro experiments were performed in triplicate. Linear mixed effects models were used to evaluate mean differences in food intake and weight between groups. Models included fixed group and time point effects, as well as random mouse effects to account for repeated measurements. *P* values of less than 0.05 were considered statistically significant. All statistical tests were two sided.

RESULTS

Effect of dietary ω-3 FAs on tumor growth and immune cells in orthotopic MycCap-Gluc tumors

Tumor growth (measured by weekly blood luminescence) and mean final tumor weight were significantly decreased in mice fed ω −3 vs the ω-6 diet (Fig. 1A, B). There was no difference in caloric intake between the groups (Supplementary Fig. 2A). At the later time points in the experiment, the body weight was significantly higher in the ω-6 vs the ω-3 group (Supplementary Fig. 2B). The final tumor weights correlated with the mouse weights at the time of sacrifice. Immune cell infiltration in the orthotopic tumors was determined by flow cytometry. Mice fed the ω-3 diet had fewer F4/80+CD11b+ total macrophages and fewer F4/80+CD206+M2 polarized macrophages than mice fed the ω-6 diet (Fig. 2A). There was no statistically significant difference between mice fed the ω-3 diet or ω-6 diet in cell numbers of other immune cells such as F4/80+CD68+M1 polarized macrophages, CD11b+Gr1+MDSCs, F4/80-CD11b+Gr1+neutrophils, CD8+ or CD4+ T cells, and B220+ B cells (Fig. 2A). Gene expression of M2-like macrophage markers CD206 and colony stimulating factor 1 receptor (CSF-1R) were significantly decreased in tumors from the ω-3 compared to the ω-6 group (Fig. 2B). There was no significant difference in gene expression of M1-like markers CD68, IL-6, iNOS, between the groups, except for TNFα, which was significantly decreased in the ω-3 compared to ω-6 group (Fig. 2B).

Effect of DHA on M2 macrophage migration in an ex-vivo model

Bone marrow-derived macrophages (BMDMs) from FVB mice were induced to the M2 phenotype with MycCaP conditioned medium (CM) and L929 CM treatment. BMDM

polarization to the M2 phenotype was confirmed by an increase in gene expression of CD206 and Arg1 (Supplementary Fig. 3). Co-culture of the M2 polarized BMDMs with MycCap cells significantly increased migration of the macrophages through the matrigel layer (Fig. 3). Treatment of MycCap cells with DHA significantly decreased migration of M2 polarized BMDMs by ~44 and 57% at concentrations of 25 and 50 μM, respectively.

Effect of GPR120 knockout on DHA inhibition of M2 macrophage-induced angiogenesis

To investigate potential anticancer mechanisms of ω-3 FAs, we measured gene expression of angiogenesis factors in the orthotopic tumors. Gene expression of angiogenesis related molecules HGF, platelet-derived growth factor (PDGF), EGF and MMP-9 decreased in orthotopic tumors in mice fed the ω-3 vs the ω-6 diet, and there was a trend ($p = 0.06$) for a decrease in CD31 (Fig. 4A). We next used in vitro capillary-like tube structure formation assays to further examine the anti-angiogenic activity of ω-3 FAs and dependence on GPR120. Conditioned media (CM) from M2 polarized BMDMs from WT and GPR120 KO mice increased tube formation of murine 2H-11 cells (Fig. 4B). Whereas DHA (25 and 50 μM) treatment of M2 polarized BMDMs (from WT mice) significantly reduced CM-induced tube formation of 2H-11 cells (Fig. 4B), this was not the case for M2 polarized BMDMs from GPR120 KO mice (Fig. 4B). We saw similar findings using human THP-1 polarized M2 macrophages and human endothelial cells (HUVEC). CM from M2 polarized THP-1 cells increased tube formation of HUVEC cells (Fig. 4C). DHA treatment (50 μM) of M2 polarized THP-1 cells reduced CM-induced tube formation of HUVEC cells, whereas this was not the case with CM from GPR120 depleted M2 polarized THP-1 cells. As a control, DHA at the same concentrations did not directly inhibit tube formation of 2H-11 cells (Supplementary Fig. 4).

Effect of GPR120 knockout on DHA activation of T cells

To investigate if ω-3 FAs inhibit the immunosuppressive effects of tumor associated macrophages and are dependent on GPR120, we examined isolated M2-like macrophages from a prior feeding experiment in which subcutaneous MyCaP tumors were grown in immunocompetent WT and global GPR120KO mice fed an ω-3 or ω-6 diet [6]. PD-L1 expression in tumor infiltrating M2-like macrophages was significantly decreased in the ω-3 diet group relative to the ω-6 group in the WT mice, but this was not the case in GPR120KO mice (Supplementary Fig. 5). PD-L2 gene expression in tumor infiltrating M2-like macrophages was not significantly reduced by an ω-3 (relative to an ω-6) diet (Supplementary Fig. 5). To further examine if ω-3 FAs inhibit the immunosuppressive effects of M2 macrophages and are dependent on GPR120, we used two T cell activation assays in which activated T cells were co-cultured with M2 macrophages from WT and GPR120 KO mouse bone marrow. In the T cell INF-γ assay, co-culture of activated T cells with M2 polarized macrophages from WT mice significantly suppressed T cell activation. Inhibition of both markers of T cell activation was reversed when M2 polarized macrophages were pretreated with 50 μM of DHA (Fig. 5A, B). In both T cell activation assays, DHA treated M2 polarized macrophages from GPR120KO mice did not reverse the suppression (Fig. 5A, B).

DISCUSSION

Omega-3 FA diets have previously been reported to inhibit prostate cancer development and progression in preclinical models, but have not been tested in an orthotopic model [1-8]. Orthotopic tumor growth occurs in the local microenvironment of the prostate and may represent a more physiologic model for angiogenesis and other biological pathways as compared to subcutaneous tumor models [35-37]. We found that an ω-3 diet (as compared to an ω-6 diet) significantly delayed prostate cancer progresssion of orthotopic MycCaP tumors in immunocompetent mice. As previously demonstrated in subcutaneous allograft tumors, we also found a significant decrease in the number of tumor infiltrating M2-like macrophages in tumors from the ω-3 relative to the ω-6 diet group [6].

M2-like macrophages play a key role in prostate cancer progression by promoting tumor invasion, angiogenesis, and immunosuppression [24]. In the present study, dietary ω-3 FAs significantly decreased expression of key regulators of angiogenesis including PDGF, hepatocyte growth factor, and epidermal growth factor (EGF) in the orthotopic tumors, and there was a trend for decreased expression of CD31, a marker of angiogenesis [41]. Gene expression of vascular endothelial growth factor (VEGF), a commonly investigated stimulator of angiogenesis, however, was not inhibited. This is in agreement with other in vitro and in vivo findings of suppression of neo-vascularization without suppression of VEGF [42], although a prior study reported reduced expression of VEGF in castration resistant tumor tissue in fish oil-fed mice [7]. VEGF is mainly secreted by M1-like macrophages and epithelial cells and the ω-3 diet did not change the number of M1-like macrophages in our present study, though M1-like macrophages were increased in our prior study of castrate resistant tumors [6, 43]. Potential mechanisms for how M2-like TAMs enhance angiogenesis in the tumor microenvironment include induction of dioxygenase 12-lipoxygenase (12-LOX), converting arachidonic acid into 12-hydroxyeicosatetraenoic acid (12-HETE) and production of other pro-angiogenic cytokines [44]. Using an ex-vivo co-culture assay in which M2-like BMDMs were co-cultured with MyccCap cells, we found that DHA (an ω-3 FA) inhibited M2 macrophage migration towards MyCaP cells. Since CSF-1R gene expression was significantly decreased in orthotopic tumor tissue from the ω-3 group, we hypothesize that ω-3 FAs target the CSF-1/CSF-1R cytokine axis responsible for attracting tumor associated macrophages to the tumor microenvironment. Taken together, these data support a potential role for dietary ω-3 FAs for inhibiting tumor infiltrating M2-like macrophages and M2-like macrophage-induced angiogenesis.

Dietary ω-3 FAs may have anticancer effects through multiple mechanisms including inhibition of inflammation by regulation of cyclooxygenases and lipoxygenases, formation of resolvins, and suppression of inflammatory mediators such as toll like receptors, as well as inhibition of proliferation and induction of apotosis through modulating signal transcription by incorporation into membrane phospholipids [45]. Recently, in a preclinical model, the anticancer effects of ω-3 FAs were reported to be dependent on functional host GPR120, although the responsible host cell type(s) are yet to be defined [6]. GPR120 is a receptor for ω-3 FAs on macrophages, adipocytes and other cells [31, 32, 46].GPR120 status in the host is of interest as it may potentially predict responsiveness to an ω-3 based diet [6]. In a small prospective pre-prostatectomy trial in men with prostate cancer, greater GPR120

expression in prostate stroma was positively associated with greater antiproliferative effects of an ω-3 based diet [6]. Based on these findings, in the present study we sought to determine if ω-3 FA inhibition of angiogenesis and immunosuppression were dependent on GPR120. We found this to be the case using ex-vivo assays in which M2-derived macrophages were derived from wild-type or global GPR120 KO mice. Based on these findings, human trials are warranted evaluating if M-2 like macrophage GPR120 expression predicts antiprostate cancer effects of ω-3 diets. A trial addressing this is ongoing in men on active surveillance for prostate cancer (clinicaltrials.gov: NCT02176902).

Tumor associated macrophages are known to be immunosuppressive through a number of mechanisms including cell surface ligands PD-L1 and PD-L2 [47]. Infiltration of tumor associated macrophages adversely affects prognosis in a number of solid tumors including breast, gastric, and prostate cancer [47]. In our study there was reduced infiltration of M2-like macrophages (in the ω-3 vs. ω-6 group) in the orthotopic tumors, though there was no increase in T-cell infiltration. Likewise, the effect of DHA on enhancing T-cell proliferation (via inhibition of BMDM's) was minimal, although the effect of DHA was more pronounced on T-cell interferon gamma production (T-cell activation). In addition, there was reduced PD-L1 gene expression in M2-like macrophages isolated from subcutaneous allograft tumors in mice fed an ω-3 vs. an ω-6 diet. To date, checkpoint inhibitor therapy has not proven to be effective for the majority of cases of advanced prostate cancer, likely due to the fact that there is not an intense T-cell infiltration in prostate tumors. Gao et al. recently reported that failure of anti CTLA-4 (checkpoint inhibitor) therapy in prostate cancer was associated with M2-like macrophage infiltration with high expression of PD-L1 and VISTA as potential resistance mechanisms to the therapy [48]. Given that an ω-3 diet has inhibitory effects on M2-like macrophages and reduced expression of M2-like macrophage gene expression of PD-L1, future preclinical studies are warranted evaluating combining checkpoint inhibitor therapy with ω-3 diets.

Note that in our studies on migration, angiogenesis, and T-cell activation we used DHA as opposed to EPA. We used DHA as it was the predominate ω-3 FA in our prior prospective randomized clinical trial in which a low-fat diet supplemented with a fish oil supplement lead to reduced Ki-67 index and a reduced cell cycle gene expression score in radical prostatectomy specimens [49]. EPA is also of interest given compelling antiprostate cancer effects in preclinical and clinical studies [50, 51]. Indeed, there may be an optimal combination of DHA and EPA which should be the subject of future studies.

In summary, an ω-3 diet (as compared to an ω-6 diet) significantly delayed prostate cancer progresssion of orthotopic MycCaP tumors in immunocompetent mice and reduced the number of M2-like tumor associated macrophages. DHA (ω-3 FA) inhibition of the pro-angiogenic and immunosuppressive effects of M2 macrophages was significantly reversed in GPR120 knockout M2 macrophages, suggesting GPR120 plays a key role in the anticancer effects of ω-3 FAs. Prospective clinical trials are underway by our group and others evaluating the potential for ω-3 FAs to inhibit prostate cancer progression (clinicaltrials.gov: NCT03753334, NCT02176902, NCT02333435).

Supplementary Material

Refer to Web version on PubMed Central for supplementary material.

REFERENCES

1. Berquin IM, Min Y, Wu R, Wu J, Perry D, Cline JM, et al. Modulation of prostate cancer genetic risk by omega-3 and omega-6 fatty acids. J Clin Investig. 2007;117:1866–75. [PubMed: 17607361]

2. Kobayashi N, Barnard RJ, Henning SM, Elashoff D, Reddy ST, Cohen P, et al. Effect of altering dietary omega-6/omega-3 fatty acid ratios on prostate cancer membrane composition, cyclooxygenase-2, and prostaglandin E2. Clin Cancer Res. 2006;12:4662–70. [PubMed: 16899616]

3. Saw CL, Wu TY, Paredes-Gonzalez X, Khor TO, Pung D, Kong AN. Pharmacodynamics of fish oil: protective effects against prostate cancer in TRAMP mice fed with a high fat western diet. Asian Pac J Cancer Prev. 2011;12:3331–4. [PubMed: 22471475]

4. Lloyd JC, Masko EM, Wu C, Keenan MM, Pilla DM, Aronson WJ, et al. Fish oil slows prostate cancer xenograft growth relative to other dietary fats and is associated with decreased mitochondrial and insulin pathway gene expression. Prostate cancer prostatic Dis. 2013;16:285–91. [PubMed: 23877027]

5. Liang P, Henning SM, Schokrpur S, Wu L, Doan N, Said J, et al. Effect of dietary omega-3 fatty acids on tumor-associated macrophages and prostate cancer progression. Prostate. 2016;76:1293–302. [PubMed: 27338236]

6. Liang P, Henning SM, Guan J, Grogan T, Elashoff D, Olefsky JM, et al. Role of host GPR120 in mediating dietary omega-3 fatty acid inhibition of prostate cancer. J Natl Cancer Inst. 2019;111:52–59. [PubMed: 30202902]

7. Liang P, Henning SM, Guan J, Grogan T, Elashoff D, Cohen P, et al. Effect of dietary omega-3 fatty acids on castrate-resistant prostate cancer and tumor-associated macrophages. Prostate Cancer Prostatic Dis. 2020;23:127–35. [PubMed: 31439889]

8. Gevariya N, Besancon M, Robitaille K, Picard V, Diabate L, Alesawi A, et al. Omega-3 fatty acids decrease prostate cancer progression associated with an anti-tumor immune response in eugonadal and castrated mice. Prostate. 2019;79:9–20. [PubMed: 30073695]

9. Leitzmann MF, Stampfer MJ, Michaud DS, Augustsson K, Colditz GC, Willett WC, et al. Dietary intake of n-3 and n-6 fatty acids and the risk of prostate cancer. Am J Clin Nutr. 2004;80:204–16. [PubMed: 15213050]

10. Augustsson K, Michaud DS, Rimm EB, Leitzmann MF, Stampfer MJ, Willett WC, et al. A prospective study of intake of fish and marine fatty acids and prostate cancer. Cancer Epidemiol Biomark Prev. 2003;12:64–67.

11. Lovegrove C, Ahmed K, Challacombe B, Khan MS, Popert R, Dasgupta P. Systematic review of prostate cancer risk and association with consumption of fish and fish-oils: analysis of 495,321 participants. Int J Clin Pr. 2015;69:87–105.

12. Norrish AE, Skeaff CM, Arribas GL, Sharpe SJ, Jackson RT. Prostate cancer risk and consumption of fish oils: a dietary biomarker-based case-control study. Br J Cancer. 1999;81:1238–42. [PubMed: 10584888]

13. Brasky TM, Darke AK, Song X, Tangen CM, Goodman PJ, Thompson IM, et al. Plasma phospholipid fatty acids and prostate cancer risk in the SELECT trial. J Natl Cancer Inst. 2013;105:1132–41. [PubMed: 23843441]

14. Brasky TM, Till C, White E, Neuhouser ML, Song X, Goodman P, et al. Serum phospholipid fatty acids and prostate cancer risk: results from the prostate cancer prevention trial. Am J Epidemiol. 2011;173:1429–39. [PubMed: 21518693]

15. MacLean CH, Newberry SJ, Mojica WA, Khanna P, Issa AM, Suttorp MJ, et al. Effects of omega-3 fatty acids on cancer risk: a systematic review. JAMA. 2006;295:403–15. [PubMed: 16434631]

16. Zhao Z, Reinstatler L, Klaassen Z, Xu Y, Yang X, Madi R, et al. The association of fatty acid levels and gleason grade among men undergoing radical prostatectomy. PloS ONE. 2016;11:e0166594. [PubMed: 27880795]

17. Moussa H, Nguile-Makao M, Robitaille K, Guertin MH, Allaire J, Pelletier JF, et al. Omega-3 fatty acids survey in men under active surveillance for prostate cancer: from intake to prostate tissue level. Nutrients. 2019;11:7.

18. Moreel X, Allaire J, Leger C, Caron A, Labonte ME, Lamarche B, et al. Prostatic and dietary omega-3 fatty acids and prostate cancer progression during active surveillance. Cancer Prev Res. 2014;7:766–76.

19. Galet C, Gollapudi K, Stepanian S, Byrd JB, Henning SM, Grogan T, et al. Effect of a low-fat fish oil diet on proinflammatory eicosanoids and cell-cycle progression score in men undergoing radical prostatectomy. Cancer Prev Res. 2014;7:97–104.

20. Freitas RDS, Campos MM. Protective effects of omega-3 fatty acids in cancer-related complications. Nutrients. 2019;11:945.

21. Fang LY, Izumi K, Lai KP, Liang L, Li L, Miyamoto H, et al. Infiltrating macrophages promote prostate tumorigenesis via modulating androgen receptor-mediated CCL4-STAT3 signaling. Cancer Res. 2013;73:5633–46. [PubMed: 23878190]

22. Maolake A, Izumi K, Shigehara K, Natsagdorj A, Iwamoto H, Kadomoto S, et al. Tumor-associated macrophages promote prostate cancer migration through activation of the CCL22-CCR4 axis. Oncotarget. 2017;8:9739–51. [PubMed: 28039457]

23. Escamilla J, Schokrpur S, Liu C, Priceman SJ, Moughon D, Jiang Z, et al. CSF1 receptor targeting in prostate cancer reverses macrophage-mediated resistance to androgen blockade therapy. Cancer Res. 2015;75:950–62. [PubMed: 25736687]

24. Noy R, Pollard JW. Tumor-associated macrophages: from mechanisms to therapy. Immunity. 2014;41:49–61. [PubMed: 25035953]

25. Vinnakota K, Zhang Y, Selvanesan BC, Topi G, Salim T, Sand-Dejmek J, et al. M2-like macrophages induce colon cancer cell invasion via matrix metalloproteinases. J Cell Physiol. 2017;232:3468–80. [PubMed: 28098359]

26. Huber S, Hoffmann R, Muskens F, Voehringer D. Alternatively activated macrophages inhibit T-cell proliferation by Stat6-dependent expression of PD-L2. Blood. 2010;116:3311–20. [PubMed: 20625006]

27. Jiang C, Yuan F, Wang J, Wu L. Oral squamous cell carcinoma suppressed anti-tumor immunity through induction of PD-L1 expression on tumor-associated macrophages. Immunobiology. 2017;222:651–7. [PubMed: 28017495]

28. Lo CH, Lynch CC. Multifaceted roles for macrophages in prostate cancer skeletal metastasis. Front Endocrinol. 2018;9:247.

29. Erlandsson A, Carlsson J, Lundholm M, Falt A, Andersson SO, Andren O, et al. M2 macrophages and regulatory T cells in lethal prostate cancer. Prostate. 2019;79:363–9. [PubMed: 30500076]

30. Yuri P, Shigemura K, Kitagawa K, Hadibrata E, Risan M, Zulfiqqar A, et al. Increased tumor-associated macrophages in the prostate cancer microenvironment predicted patients' survival and responses to androgen deprivation therapies in Indonesian patients cohort. Prostate Int. 2020;8:62–69. [PubMed: 32647642]

31. Oh DY, Talukdar S, Bae EJ, Imamura T, Morinaga H, Fan W, et al. GPR120 is an omega-3 fatty acid receptor mediating potent anti-inflammatory and insulin-sensitizing effects. Cell. 2010;142:687–98. [PubMed: 20813258]

32. Im DS. Functions of omega-3 fatty acids and FFA4 (GPR120) in macrophages. Eur J Pharmacol. 2016;785:36–43. [PubMed: 25987421]

33. Ichimura A, Hirasawa A, Poulain-Godefroy O, Bonnefond A, Hara T, Yengo L, et al. Dysfunction of lipid sensor GPR120 leads to obesity in both mouse and human. Nature. 2012;483:350–4. [PubMed: 22343897]

34. Poirier JG, Brennan P, McKay JD, Spitz MR, Bickeboller H, Risch A, et al. Informed genome-wide association analysis with family history as a secondary phenotype identifies novel loci of lung cancer. Genet Epidemiol. 2015;39:197–206. [PubMed: 25644374]

35. Zhang Y, Toneri M, Ma H, Yang Z, Bouvet M, Goto Y, et al. Real-time GFP intravital imaging of the differences in cellular and angiogenic behavior of subcutaneous and orthotopic nude-mouse models of human PC-3 prostate cancer. J Cell Biochem. 2016;117:2546–51. [PubMed: 27012365]

36. Zhang W, Fan W, Rachagani S, Zhou Z, Lele SM, Batra SK, et al. Comparative study of subcutaneous and orthotopic mouse models of prostate cancer: vascular perfusion, vasculature density, hypoxic burden and BB2r-targeting efficacy. Sci Rep. 2019;9:11117. [PubMed: 31366895]

37. Chung E, Yamashita H, Au P, Tannous BA, Fukumura D, Jain RK. Secreted Gaussia luciferase as a biomarker for monitoring tumor progression and treatment response of systemic metastases. PloS ONE. 2009;4:e8316. [PubMed: 20016816]

38. Cifuentes FF, Valenzuela RH, Contreras HR, Castellon EA. Development of an orthotopic model of human metastatic prostate cancer in the NOD-SCIDgamma mouse (Mus musculus) anterior prostate. Oncol Lett. 2015;10:2142–8. [PubMed: 26622809]

39. Liang P, Cheng SH, Cheng CK, Lau KM, Lin SY, Chow EY, et al. Platelet factor 4 induces cell apoptosis by inhibition of STAT3 via up-regulation of SOCS3 expression in multiple myeloma. Haematologica. 2013;98:288–95. [PubMed: 22929979]

40. Weischenfeldt J, Porse B. Bone Marrow-Derived Macrophages (BMM). Isolation and Applications. CSH protocols 2008. 10.1101/pdb.prot5080.

41. Spencer L, Mann C, Metcalfe M, Webb M, Pollard C, Spencer D, et al. The effect of omega-3 FAs on tumour angiogenesis and their therapeutic potential. Eur J cancer. 2009;45:2077–86. [PubMed: 19493674]

42. Berquin IM, Edwards IJ, Kridel SJ, Chen YQ. Polyunsaturated fatty acid metabolism in prostate cancer. Cancer Metastasis Rev. 2011;30:295–309. [PubMed: 22015690]

43. Graney PL, Ben-Shaul S, Landau S, Bajpai A, Singh B, Eager J, et al. Macrophages of diverse phenotypes drive vascularization of engineered tissues. Sci Adv. 2020;6:eaay6391. [PubMed: 32494664]

44. Mi S, Qu Y, Chen X, Wen Z, Chen P, Cheng Y. Radiotherapy increases 12-LOX and CCL5 levels in esophageal cancer cells and promotes cancer metastasis via THP-1-derived macrophages. OncoTargets Ther. 2020;13:7719–33.

45. Gu Z, Suburu J, Chen H, Chen YQ. Mechanisms of omega-3 polyunsaturated fatty acids in prostate cancer prevention. BioMed Res Int. 2013;2013:824563. [PubMed: 23762859]

46. Ren Z, Chen L, Wang Y, Wei X, Zeng S, Zheng Y, et al. Activation of the omega-3 fatty acid receptor GPR120 protects against focal cerebral ischemic injury by preventing inflammation and apoptosis in mice. J Immunol. 2019;202:747–59. [PubMed: 30598514]

47. Cassetta L, Kitamura T. Targeting tumor-associated macrophages as a potential strategy to enhance the response to immune checkpoint inhibitors. Front Cell Dev Biol. 2018;6:38. [PubMed: 29670880]

48. Gao J, Ward JF, Pettaway CA, Shi LZ, Subudhi SK, Vence LM, et al. VISTA is an inhibitory immune checkpoint that is increased after ipilimumab therapy in patients with prostate cancer. Nat Med. 2017;23:551–5. [PubMed: 28346412]

49. Aronson WJ, Kobayashi N, Barnard RJ, Henning S, Huang M, Jardack PM, et al. Phase II prospective randomized trial of a low-fat diet with fish oil supplementation in men undergoing radical prostatectomy. Cancer Prev Res. 2011;4:2062–71.

50. Gevariya N, Lachance G, Robitaille K, Joly Beauparlant C, Beaudoin L, Fournier E, et al. Omega-3 eicosapentaenoic acid reduces prostate tumor vascularity. Mol Cancer Res. 2021;19:516–27. [PubMed: 33262291]

51. Bilodeau JF, Gevariya N, Larose J, Robitaille K, Roy J, Oger C, et al. Long chain omega-3 fatty acids and their oxidized metabolites are associated with reduced prostate tumor growth. Prostaglandins Leukotrienes Essent Fat Acids. 2021;164:102215.
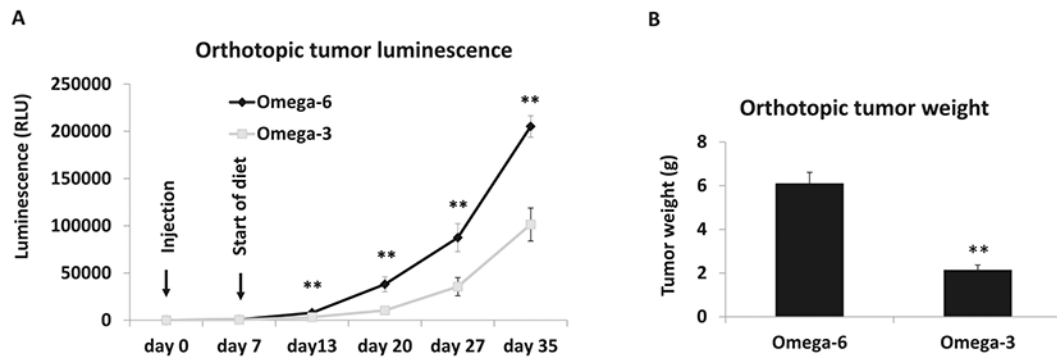
Fig. 1. The effect of dietary omega-3 fatty acids on MycCap-Gluc (Gaussia luciferase labeled) allografts in FVB mice.

Eight-week-old male immunocompetent FVB mice were fed an AIN93G diet for 1 week before orthotopic injection of 5×10^5 MycCaP-Gluc cells to the anterior prostate. When luminescence readings from serum reached 130 relative light units (RLUs), mice were randomly assigned to either the ω-3 or ω-6 diet ($n = 10$ for ω-6 diet; $n = 12$ for ω-3 diet). **A** Blood was collected every week and Gluc activity measured using a luminometer. **B** Tumor weight at day 35. Data are presented as mean ± SEM. $*p < 0.05$, $**p < 0.01$.
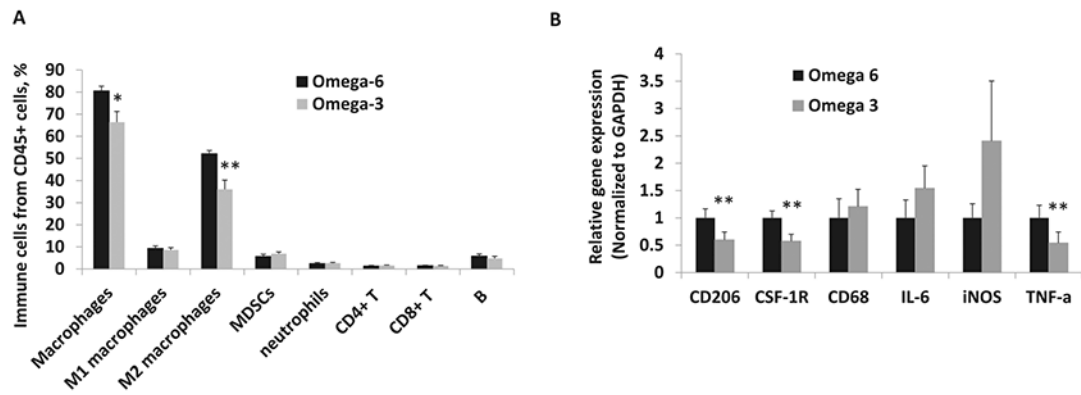
Fig. 2. Effect of dietary omega-3 fatty acids on immune cell infiltration and CD206 and CSF-1R gene expression in MycCap-Gluc orthotopic tumors.
A Immune cell infiltration in tumor tissue by flow cytometry. **B** Gene expression of M2 macrophage markers was analyzed by quantitative real-time polymerase chain reaction in tumor tissue ($n = 10$ for ω-6 diet; $n = 12$ for ω-3 diet). Data are presented as mean ± SEM. $*p < 0.05$, $**p < 0.01$.
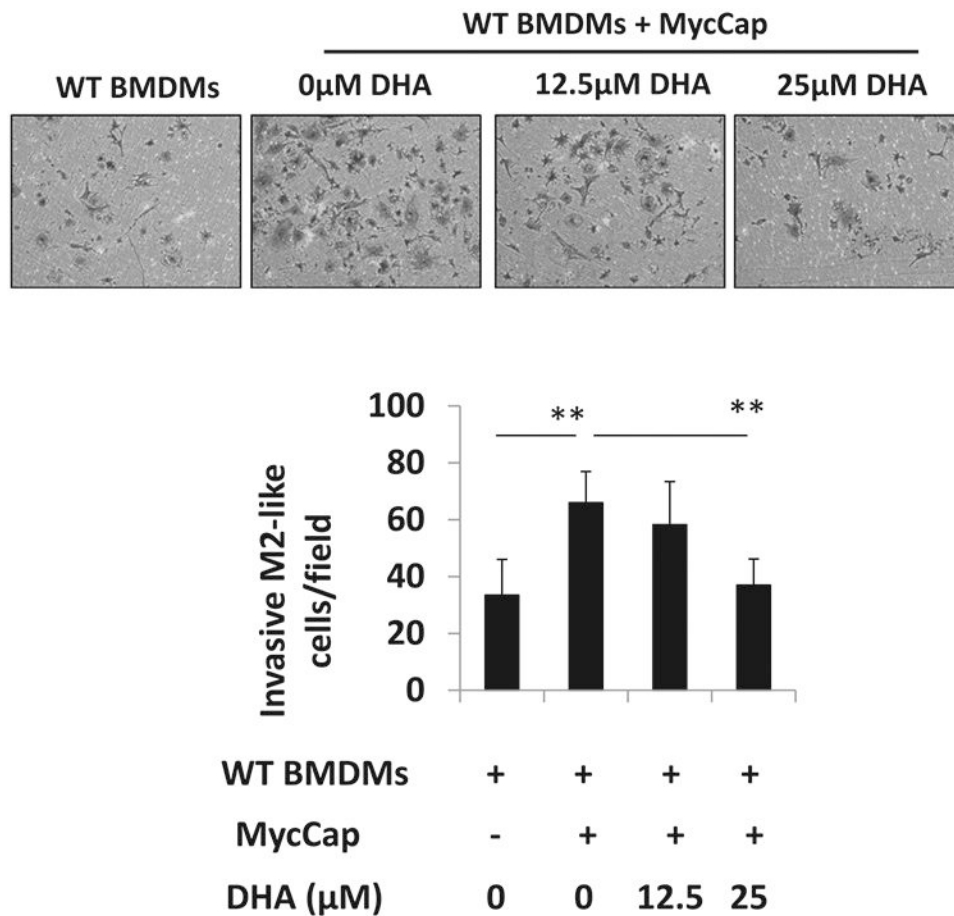
Fig. 3. Effect of docosahexaenoic acid (DHA) on migration of bone marrow derived macrophages (BMDMs) co-cultured with MycCap cells.

Bone marrow cells were isolated from WT mice and induced to M2-like BMDMs by supplementation with 80% MycCaP CM and 20% L929 CM for 7 days. MycCap cells were treated with DHA and co-cultured with WT or BMDMs using Matrigel-coated inserts. The invasive BMDMs were fixed and stained. Pictures were taken with a digital microscope (upper panel), and the numbers of invasive cells were counted in different fields (lower panel). Data are presented as mean ± SD. $*p < 0.05$, $**p < 0.01$.
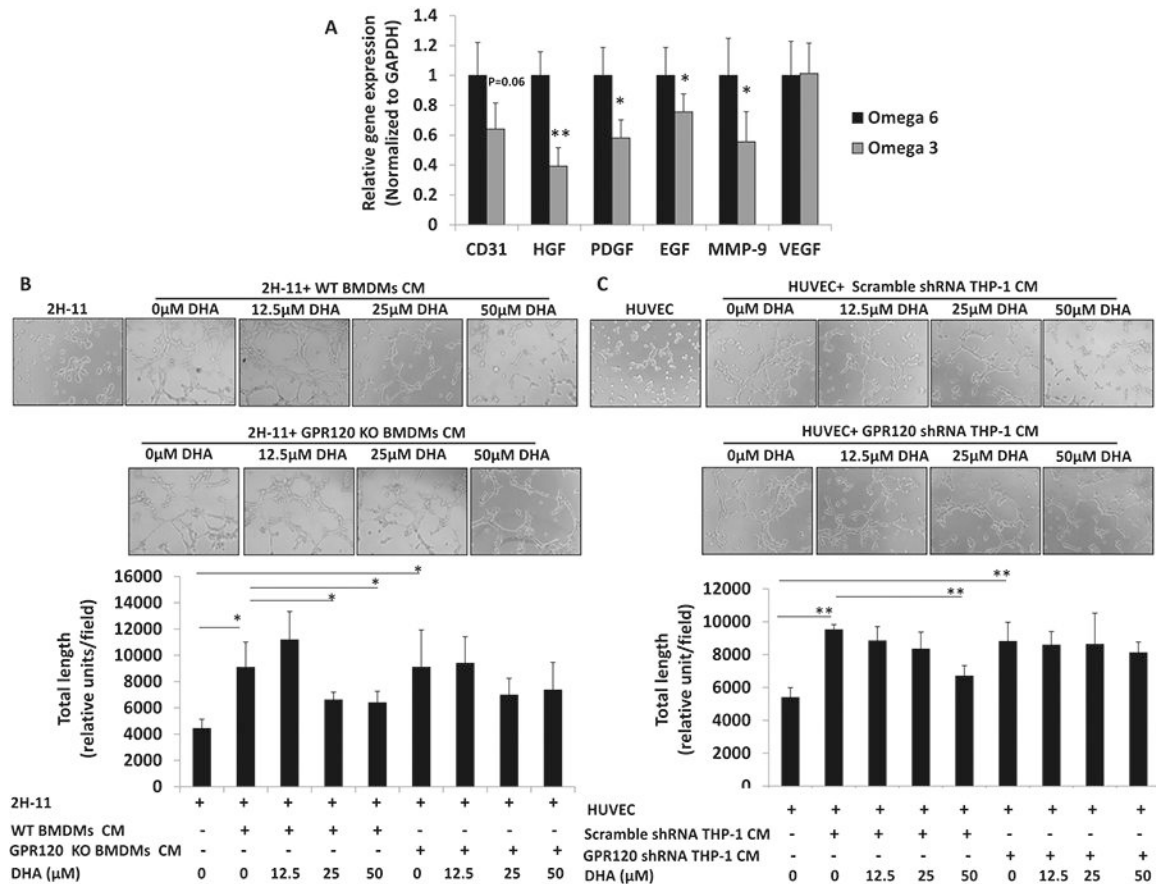
Fig. 4. The effect of omega-3 fatty acids on angiogenesis in vivo and in vitro.

A Gene expression of angiogenesis and invasion markers was analyzed by quantitative real-time polymerase chain reaction in tumor tissue ($n = 10$ for ω-6 diet; $n = 12$ for ω-3 diet). **B** Mouse endothelium 2H-11 tube formation. BMDMs were isolated from WT or GPR120 KO FVB mice and polarized to M2 macrophages as described in Fig. 3. BMDMs were then treated with DHA for 24 h. Conditioned medium (CM) was collected. 2H-11 cells were seeded in 96-well culture plates precoated with Matrigel, treated with CM for 4 h, and examined for tube formation using an inverted microscope. **C** Human endothelium cell (HUVEC) tube formation. THP-1 cells were transfected with GPR120-specific shRNA or scramble controls, then polarized to M2 cells by treatment with 320 nM PMA (Sigma). After 24 h, PMA was removed and cells stimulated with 20 ng/mL interleukin (IL)-4 (Sigma, USA) for 24 h. Cells were treated with DHA at the indicated concentrations for 24 h. CM was collected. HUVEC cells were seeded in 96-well culture plates precoated with Matrigel, treated with CM for 4 h, and examined for tube formation using an inverted microscope. For **A** data are presented as mean ± SEM. For **B**, **C**, data are presented as mean ± SD. *$p < 0.05$, **$p < 0.01$.
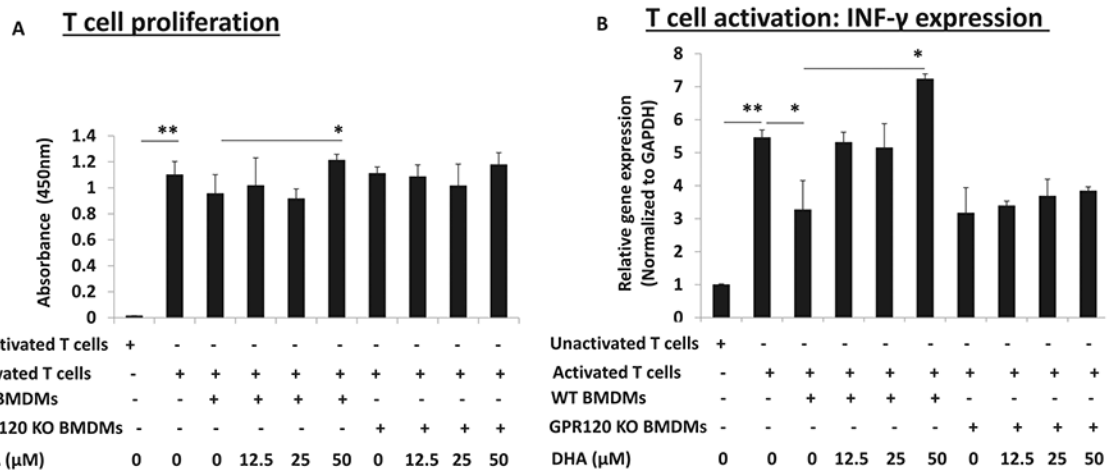
Fig. 5. Effect of DHA on T cell proliferation and INF-γ gene expression.
CD8+ T cells were isolated from spleen cells of FVB mice and stimulated with anti-CD3 and anti-CD28 antibodies to become activated T cells. BMDMs were isolated from WT or GPR120 KO FVB mice and polarized to M2 macrophages as described in Fig. 3. Activated T cells were co-cultured with WT or GPR120 KO BMDMs and treated with DHA in 96-well plates for 72 h. CD8+ T were collected and analyzed for proliferation by BrdU.1 assay (**A**) or gene expression of INF-γ by quantitative PCR (**B**). Data are presented as mean ± SD. $*p < 0.05$, $**p < 0.01$.